

# Melting and spheroidization of hexagonal boron nitride in a microwave-powered, atmospheric pressure nitrogen plasma

S. GLEIMAN

*Los Alamos National Laboratory, Los Alamos, NM 87545, USA*

*E-mail: gleiman@lanl.gov*

CHUN-KU CHEN\*, A. DATYE†

*\*Department of Chemical and Nuclear Engineering, and †Center for Micro-Engineered Materials, University of New Mexico, Albuquerque, NM 87131, USA*

J. PHILLIPS‡

*Los Alamos National Laboratory/University of New Mexico, National Lab Professor, C.M.S. C-930 Los Alamos, NM 87545, USA*

We have developed a method for producing spherically-shaped, hexagonal phase boron nitride (hBN) particles of controlled diameter in the 10–100 micron size range. Specifically, platelet-shaped hBN particles are passed as an aerosol through a microwave-generated, atmospheric pressure, nitrogen plasma. In the plasma, agglomerates formed by collisions between input hBN particles, melt and form spheres. We postulate that this unprecedented process takes place in the unique environment of a plasma containing a high N-atom concentration, because in such an environment the decomposition temperature can be raised above the melting temperature. Indeed, given the following relationship (V. L. Vinogradov and Kostanovskii, *Teplofizika Vysokikh Temperatur* **29** (1991) 1112):  $\text{BN}_{(\text{condensed})} \leftrightarrow \text{B}_{(\text{gas})} + \text{N}_{(\text{gas})}$ . Standard equilibrium thermodynamics indicate that the decomposition temperature of hBN is increased in the presence of high concentrations of N atoms. We postulate that in our plasma system the N atom concentration is high enough to raise the decomposition temperature above the (undetermined) melting temperature.

© 2002 Kluwer Academic Publishers

## 1. Introduction

Both hexagonal and cubic boron nitride have unique properties and related applications. The hexagonal phase (hBN) is well suited for use as a heat transfer agent in some applications because it has the highest thermal conductivity of any ceramic. The cubic phase of BN (cBN) is the second hardest material, after diamond, but its stability in aggressive oxidizing environments make it the preferred choice in high-temperature tool applications.

Potentially the most significant application of the novel material described herein, spherical-shaped, micron-scale, hexagonal-phase BN, will be as a filler in integrated circuit (IC) packages. Various strategies have been devised in recent years to accelerate heat removal from ICs (e.g., fans, heat pipes). Yet, it is generally agreed that as chips become larger and consume more power, thermal management will require additional technological advances. This includes the replacement of the current IC package filler material, silica (an insulator), with a high thermal conductivity,

low thermal expansion coefficient material such as BN [1]. Although BN clearly has the best properties for this application, it is not presently used because it cannot be generated in spherical form. Polymer melts containing platelet-shaped BN have a viscosity too high for use in injection molding processes often employed to create IC packages.

Melting hBN was thought to require severe temperatures (>3000 K) and pressures (>2.0 GPa). Several BN phase diagrams [2, 3–8] have been proposed since Wentorf [9] originally described a melting line for BN. Although refinements have been made to the phase diagram, including a more exact measure of the hBN-L-V triple point [8], advances have been few in the low-pressure region (~1 atm.) of the P-T diagram where we have demonstrated melting of BN. We show in the present work a means to create hBN in spheres in the size range of 10 to 100 microns from platelet hBN precursor material using an atmospheric pressure, microwave-powered nitrogen plasma.

‡Author to whom all correspondence should be addressed.

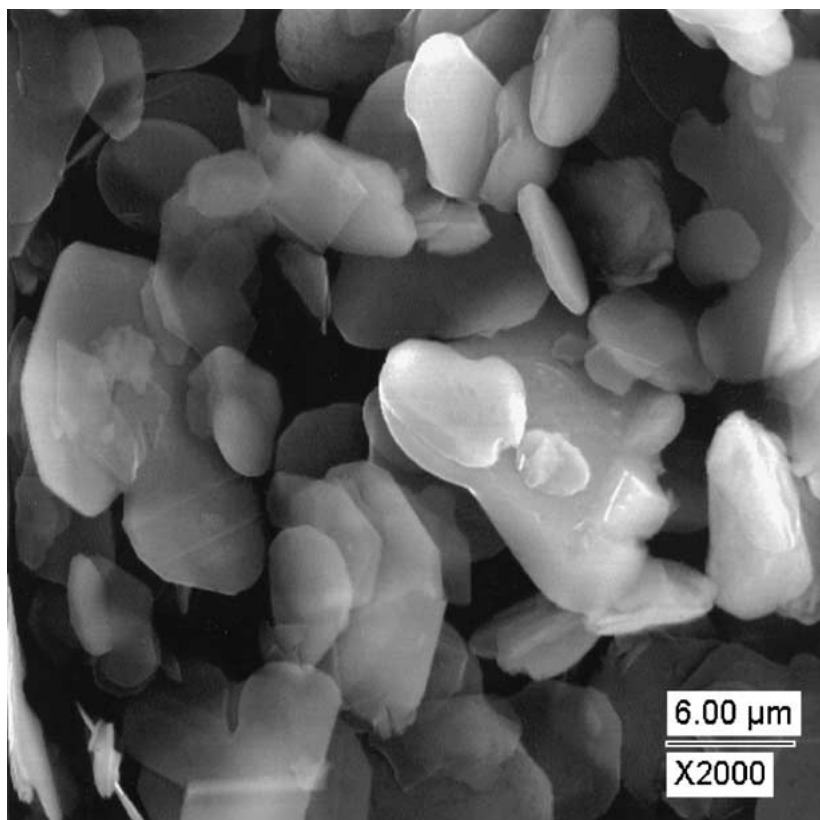


Figure 1 hBN precursor particles from Advanced Ceramics Corporation. Note the platelet shape. The original particle volume is approximately  $85 \mu\text{m}^3$  with an average surface dimension of  $5 \mu\text{m}$  across.

## 2. Experimental

The two key components to the system employed in the present work, a low-power, atmospheric pressure, gas-flow microwave plasma, and a particle feeder of novel design, are described in detail elsewhere [10–13]. In brief, to generate a plasma, two gas streams are fed through a quartz torch (cylinder, 19 mm ID) which passes through a microwave (2.45 GHz) waveguide ( $\text{TE}_{10}$ ). One of the streams (“plasma gas”) is passed through the main body of the torch, and the second stream (“aerosol gas” contains particles) passes through a coaxial central alumina tube (3 mm ID) that terminates within the torch. Particle concentration in the aerosol stream can be controlled using any number of particle feeder devices. In the system used in the present work, hBN precursor particles are fed to the aerosol gas via an oscillated reservoir placed just below the torch entrance. Particles are suspended in the gas stream, producing a cloud of particles, some of which are injected into the torch.

In most cases reported herein the precursor particles were “platelets” of hBN (Fig. 1) [14] that form a white powder in bulk and tend to compact easily. The average volume of a precursor particle is about  $85 \mu\text{m}^3$ . It was found, however, that the precise nature of the precursor is not critical. In a few cases, spherical BNO particles about 1 micron across were used as the feed. These were also partially converted to spherical BN particles in the  $10 \mu\text{m}$  scale size. Precursor particles were fed to the torch under several applied powers and constant plasma and aerosol gas flow rates. The mass flow rate of BN precursor powder through the plasma

torch ranged from less than 1 mg/hr to approximately 1000 mg/hr.

The use of the nitrogen plasma to generate spherical hBN was limited in practice to a range of input powers between 500 and 1500 watts. Below 500 W the nitrogen plasma was unstable and above 1500 W the torch overheated quickly. UHP nitrogen gas flow was controlled with rotameters so that the plasma gas flow rate ranged from 1.3 to 3.0 standard liters per minute (slpm) and the aerosol gas flow rate ranged from 0.06 to 1.2 slpm.

Argon plasmas, operated in the same flow rate and power ranges were also used (with UHP argon) to provide equivalent, and possibly higher plasma temperatures, but without N atoms.

Cooling water around  $5^\circ\text{C}$  was circulated throughout the plasma torch system to allow the system to be operated continuously without overheating. A simple gas handling system vented the plasma exhaust gas.

Once the feeder is turned on, hBN precursor particles and multi particle agglomerates are carried to the plasma in the aerosol gas stream. Upon injection to the plasma hot zone, some of the hBN particles and agglomerates melt and are carried out of the torch and through the plasma afterglow. Indeed, some precursor particles melt incompletely and join together with other particles (both molten particles and unmelted agglomerates). Surface tension dictates the coalescence of the molten particles into spheres. Some molten spheres may even collide to form larger spheres. Cooling rates as large as  $10^5 \text{ K/sec}$  are known to exist in the plasma afterglow; spheres and unmelted agglomerates leave the

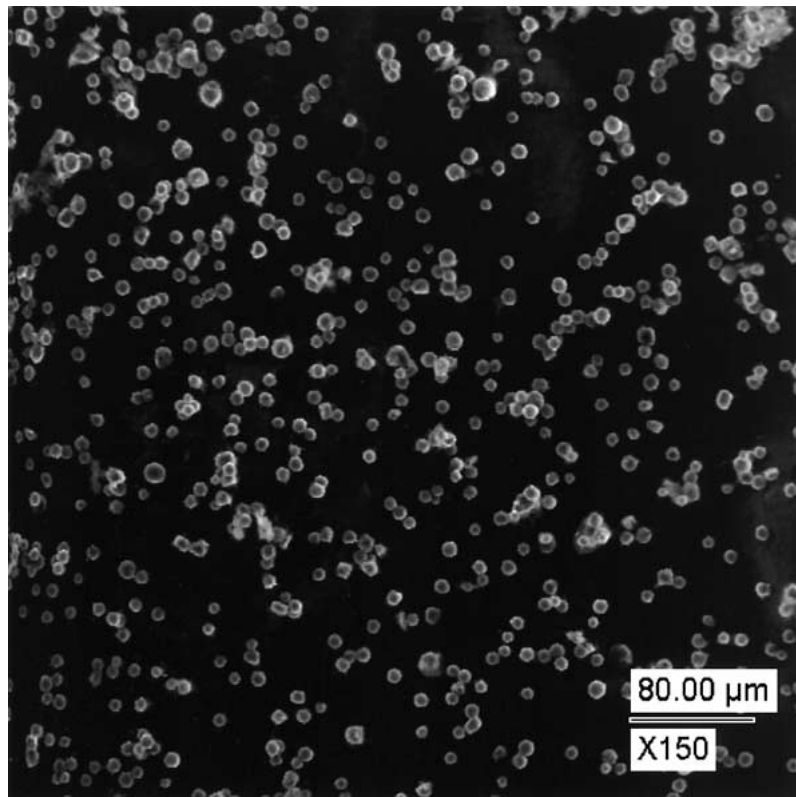
afterglow region and freeze, maintaining their shapes. The newly formed hBN spheres (and agglomerates) pass directly into the particle trap.

Visual inspection of the plasma-treated powder shows a marked difference from the white hBN precursor material. That is, the treated particles were gray

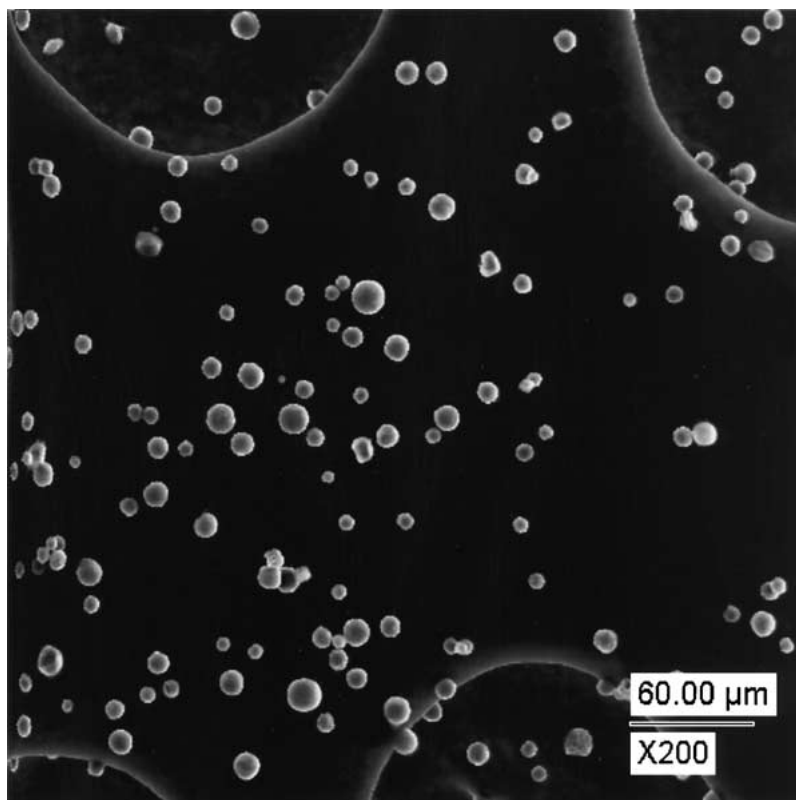
to black in color and less likely to form large particulate compacts.

### 3. Results

Examination in a scanning electron microscope (SEM) revealed remarkable material transformations as shown

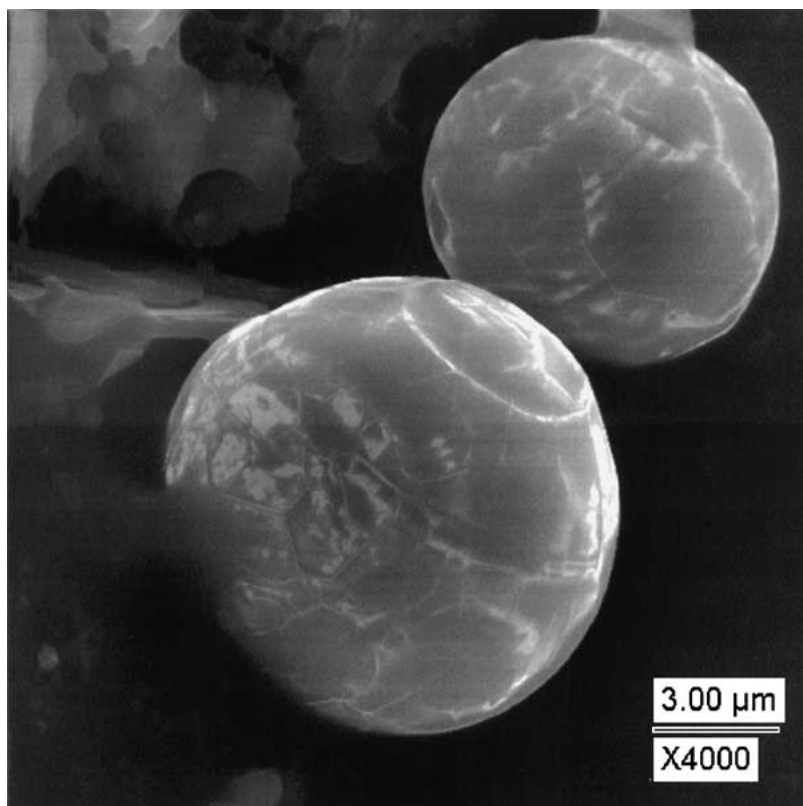


(a)

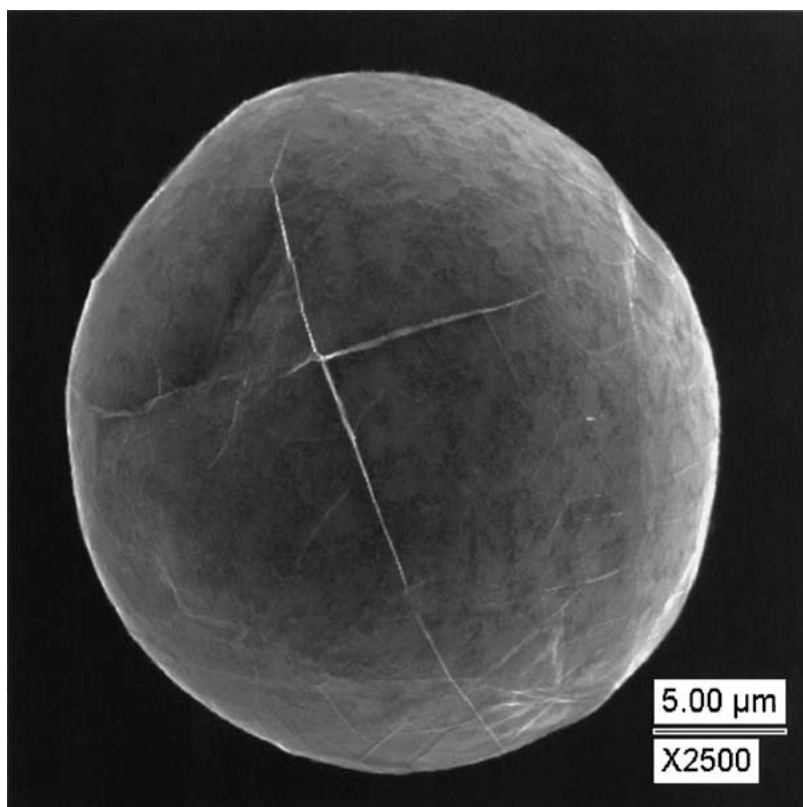


(b)

Figure 2 (a, b) SEM image of spherical hBN particles. Generally agglomerates form simultaneously with spheres, although complete spheroidization of a sample has been observed. All pictures are taken from Sample 1 (see Table I). (c) High magnification SEM image of BN spheres. Note interesting surface colorations and 'veined' appearance. (d) Single BN sphere with dramatic surface morphology. (Continued.)



(c)



(d)

Figure 2 (Continued).

in Fig. 2a–d. Under many of the operating conditions employed, spherical hBN particles were mixed with agglomerates and unconverted particles. In some cases, nearly 100% “conversion” into spheres of the precursor material was found. The fraction of material converted was found to be a very strong function of the operation parameters. Average particles volumes of the precursor

and converted particles are compared in Table I for several operating conditions.

In order to determine the composition and crystal habit of the product hBN, a number of analytical probes were used. The most compelling choice for identification of the crystal structure of the spheres was selected area diffraction (SAD) obtained with a transmission

TABLE I Average spherical particle volumes as a function of several operating conditions

Sample	Applied plasma power (watts)	Plasma gas flow rate (slpm)	Aerosol gas flow rate (slpm)	Average particle volume ( $\mu\text{m}^3$ )
1	1000	2.3440	1.2744	384.6
2	1000	1.8870	0.7228	502.4
3	800	1.8870	0.7228	395.6
4	1350	2.3440	0.7557	553.2
5	1000	1.8870	0.6900	648.9
6	1350	1.8870	0.7228	1203.5
Precursor				84.7

Average spherical particle volumes as a function of several operating conditions including applied plasma power, plasma and aerosol gas flow rates. The aerosol gas flow includes a small contribution from an Argon flow used to stabilize and increase the temperature of the plasma. This fraction is less than 15% of the total aerosol flow. Note that the precursor particle volume is at least four times smaller than the smallest average spherical particle volume measured.

electron microscope (TEM), and standard x-ray diffraction (XRD) obtained using a  $2\theta$  device with Cu  $K\alpha$  radiation.

SAD (an example is shown in Fig. 3) investigation of dozens of spherical particles showed that all were crystalline (hexagonal). All spherical particles studied produced single, sharp hexagonal diffraction patterns, precisely those expected for hexagonal BN. These studies are not considered definitive because only the edges of the particles are thin enough to pass electrons. Thus, this approach is capable of identifying only the crystal structure of the near surface region ( $\sim 1$  micron depth) of the spherical particles. Additional data were obtained from studies of polished samples in the TEM. SAD studies of

TABLE II X-Ray photoelectron spectroscopy data of precursor and product material

Atomic constituent	Precursor material assay	Plasma treated material assay
B	48	49
N	49	49
O	1	<1

X-ray photoelectron spectroscopy data indicating stoichiometric levels of boron and nitrogen with a minimum of oxygen in a plasma treated sample consisting of more than 90% spheres.

about one dozen large cross-section particles (far larger than the precursor) again revealed that the structures were those of hexagonal BN. Most diffraction patterns were dominated by a single crystal (Fig. 5), although in all cases evidence of polycrystalline structure was evident. In sum, these studies suggest that most spherical particles are polycrystalline, but that each crystal is many microns in volume.

XRD studies also showed slight a change between the input precursor particles and the samples containing spheres. The spectrum of the precursor showed classic indications of preferential orientation of hexagonal BN, consistent with “flat” particles lying parallel to the surface of the specimen holder (Fig. 4a). In contrast, the samples containing a significant fraction of spheres (Fig. 4b) had relative intensities virtually identical to that of the standard powder pattern. This would be expected for spherical particles of hBN because they would not orient relative to the specimen holder with any preferential crystal orientation.

X-ray photoelectron spectroscopy (XPS) indicated a small (<1%) oxygen content, as shown in Table II.

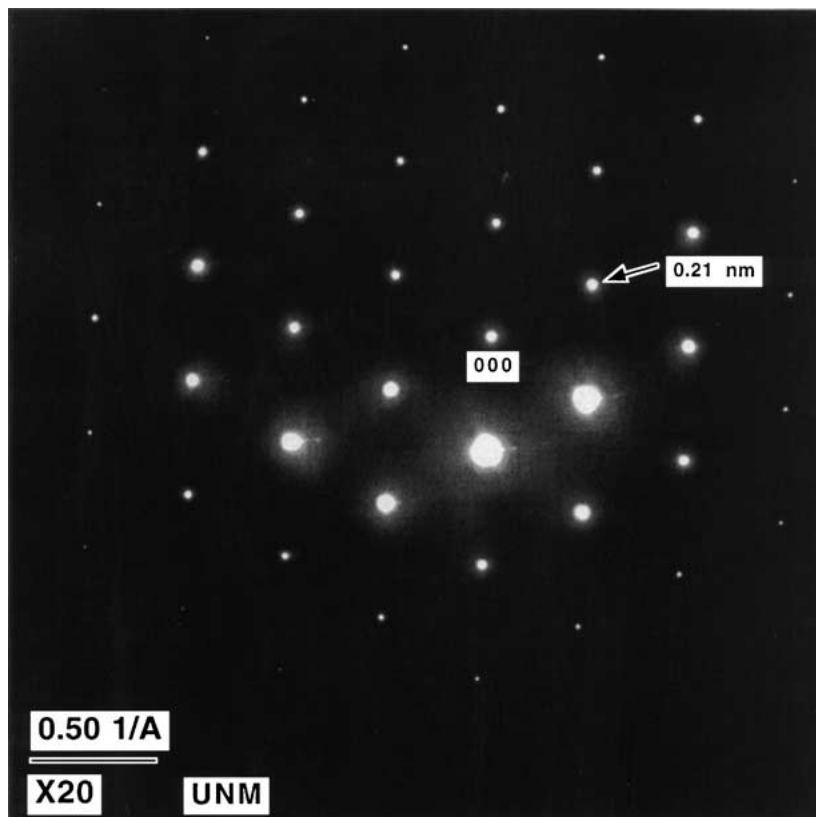
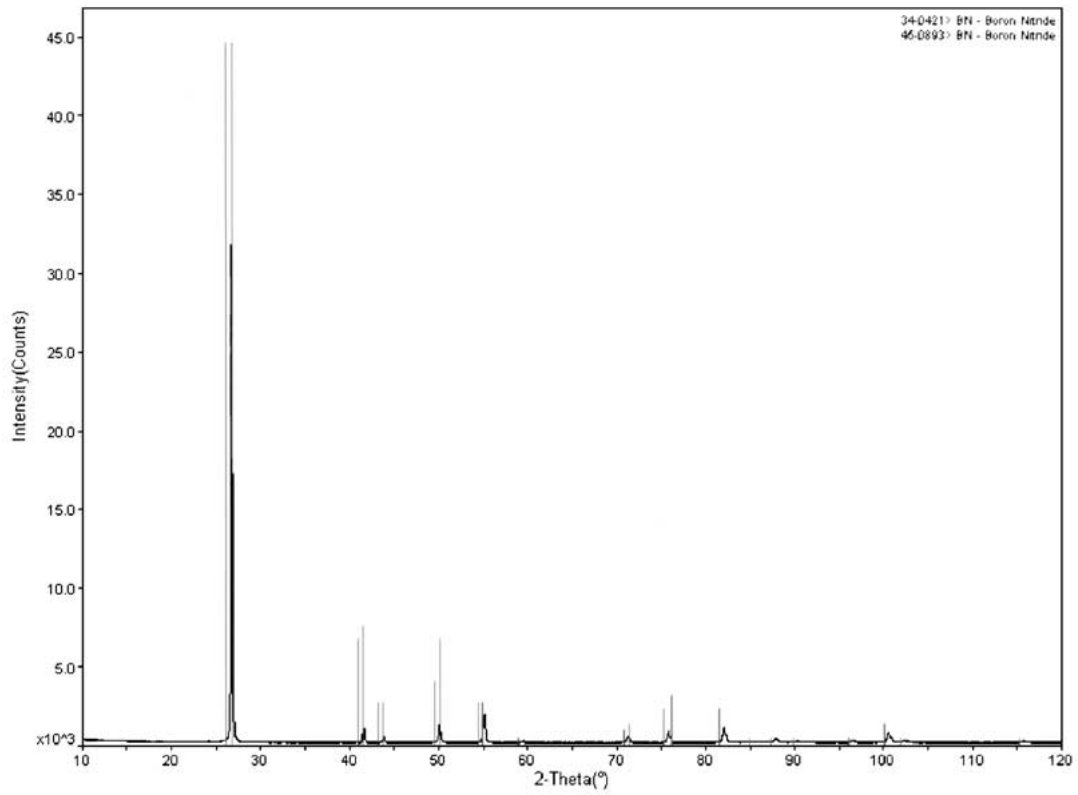
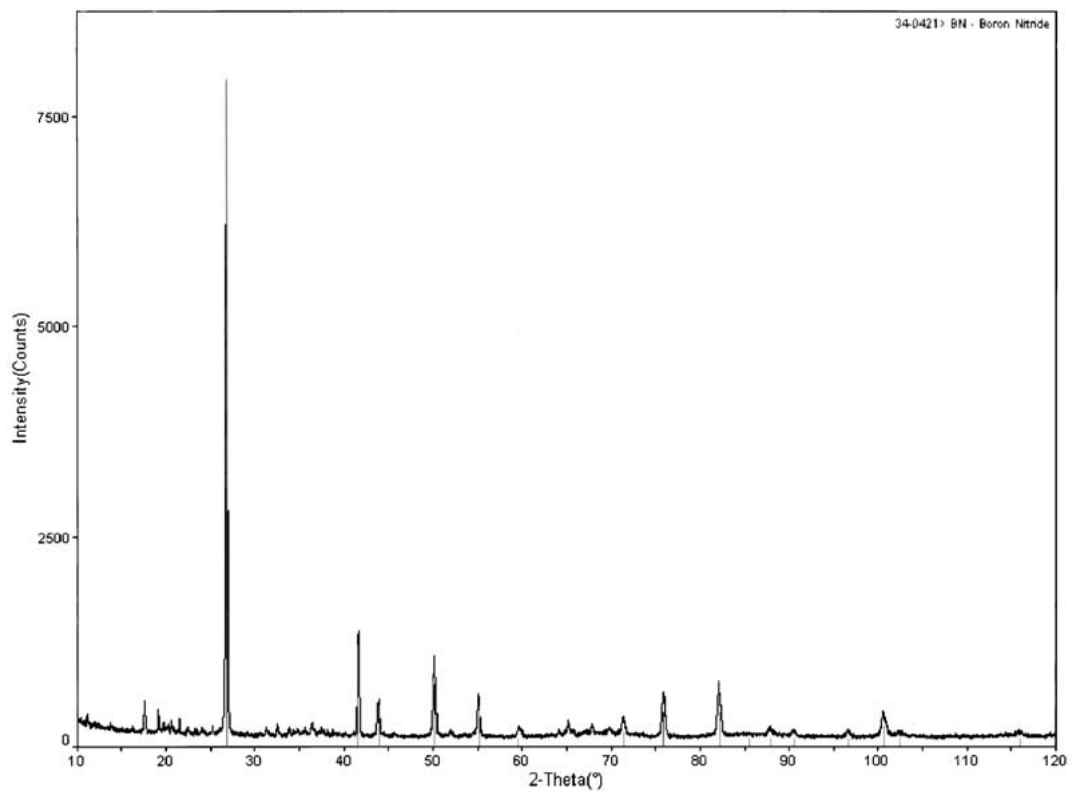


Figure 3 Selective-angle diffraction pattern of a spherical hBN particle indicating the hexagonal crystal pattern.



Earth & Planetary Sci., UNM

(a)



Earth & Planetary Sci., UNM

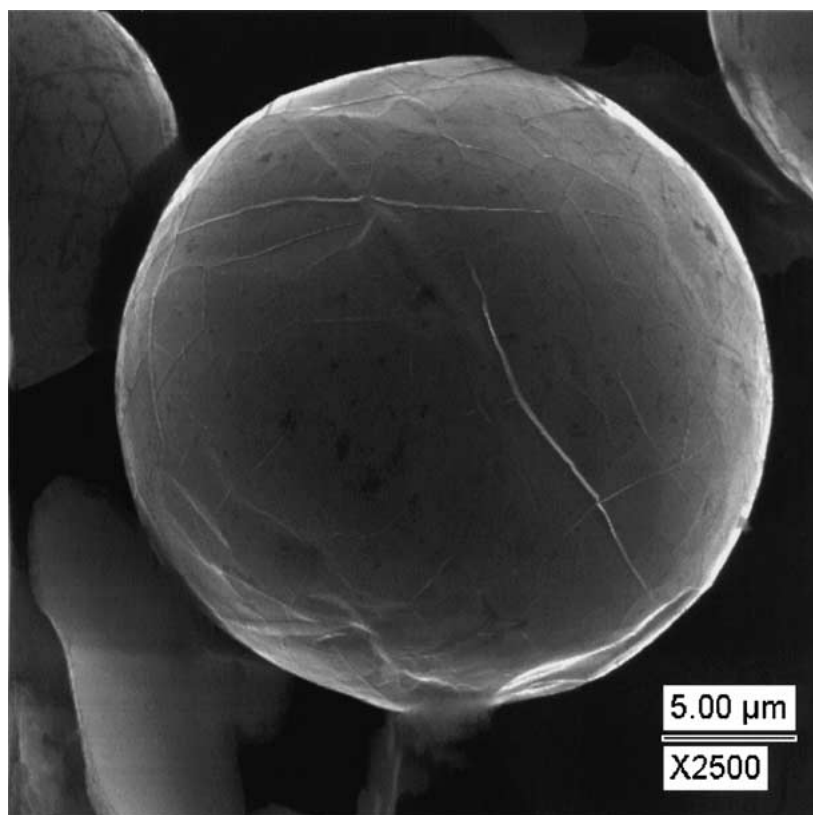
(b)

Figure 4 X-Ray diffraction patterns of samples containing precursor (top) and spherical product (bottom). There are many differences, but one of the easiest to see is the relatively stronger signal for high-angle peaks found in the spherical product.

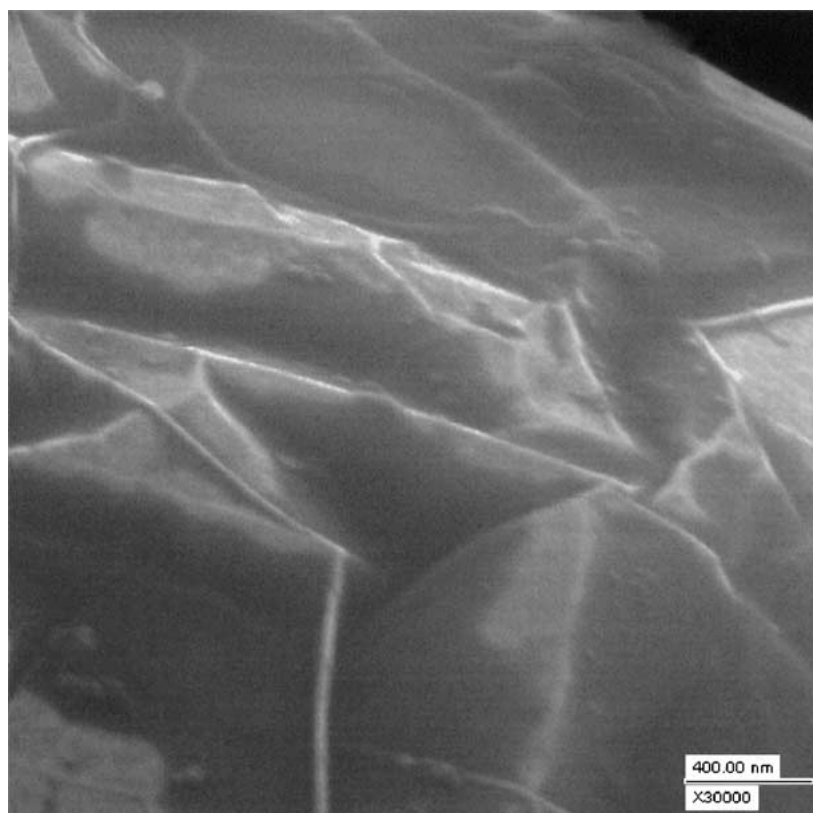
This is consistent with surface oxygen contamination possibly occurring during post processing. Moreover, XPS showed that the atomic ratios of the two species were totally consistent with stoichiometric BN.

The surface morphology of the spherical particles is not a clear function of the operating conditions at which they are produced. For instance, at

lower powers (<600 W) the spherical particle surfaces appear to be flat planes connected by sharp edges (Fig. 5a and b). Likewise, at high powers (>1000 W), the particle surfaces maintain the 'veined' morphology evident even at the highest magnification (Fig. 5c and d). In contrast, some spherical particles are morphologically "plain"; that is, the

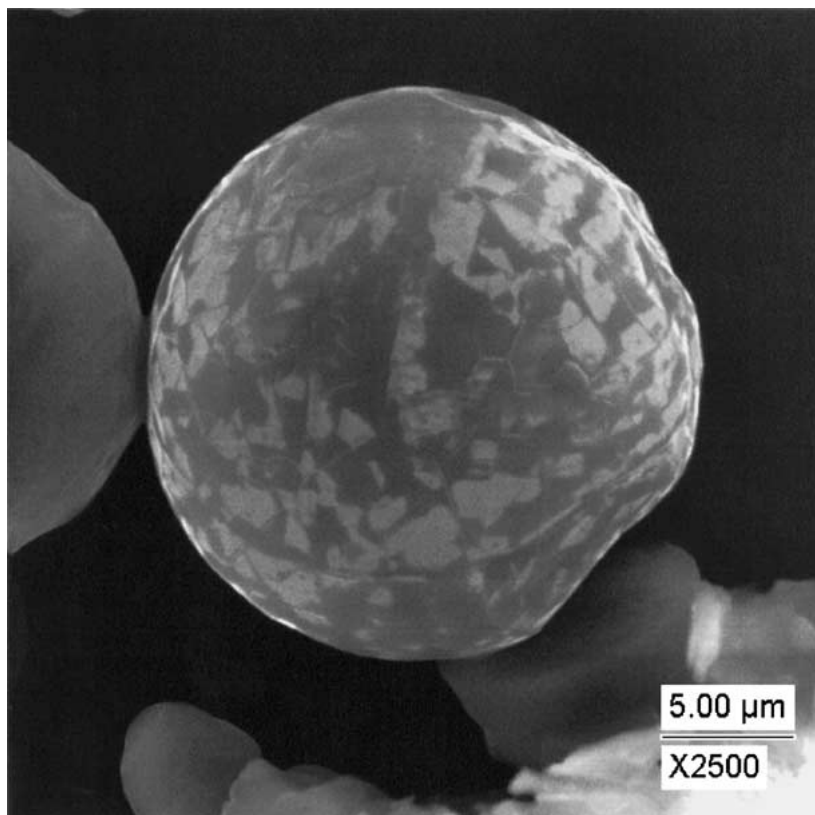


(a)

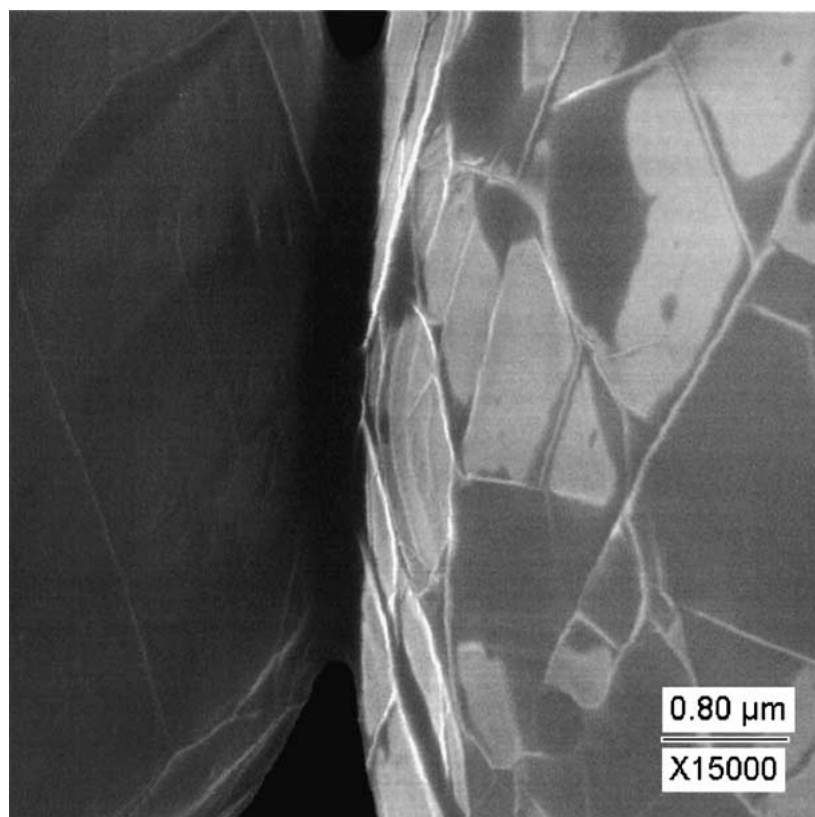


(b)

Figure 5 Investigation of sphere surface morphology. A highly textured surface is visible at higher magnifications. The origin and nature of the surface morphology, 'veined' structures and mottling, is not understood. (Continued.)



(c)



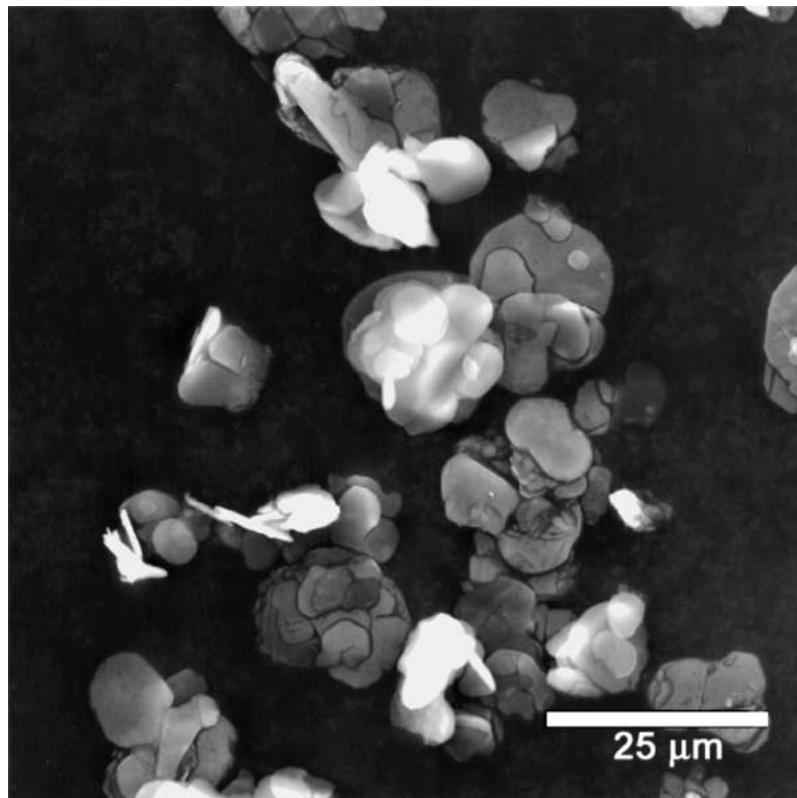
(d)

Figure 5 (Continued).

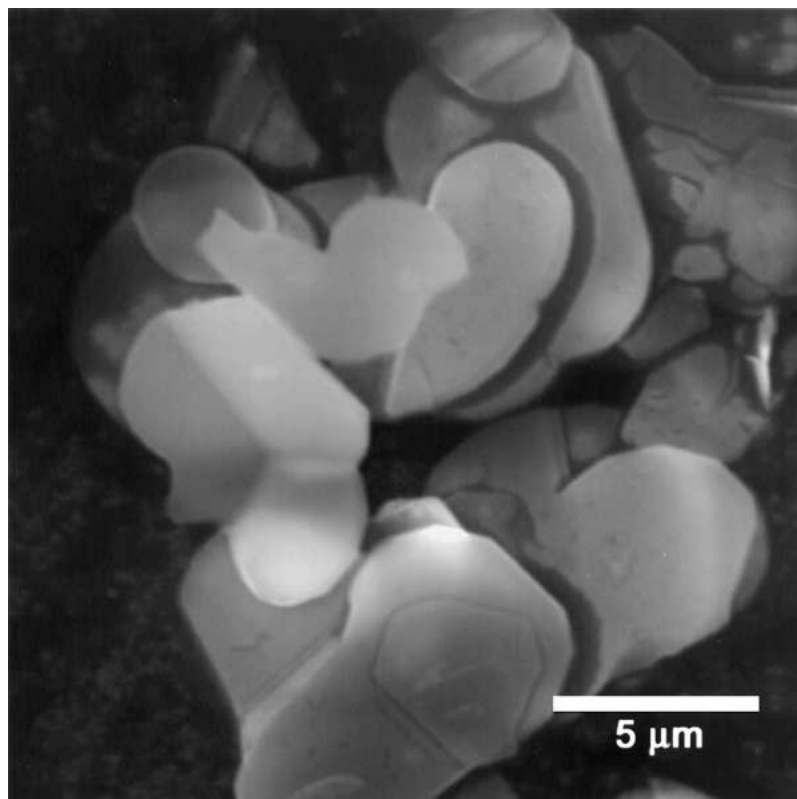
particles exhibit no discernable (through SEM investigation) morphological characteristics. Grain boundary structures are not evident in TEM measurements at any magnification in particles produced at any power.

Previous studies provide an illuminating contrast between a simple heating technique and the plasma process described herein. Spherical BN particles generated

by a chemical technique were studied using SAD, and in no case was any diffraction pattern detected, suggesting that the spherical particles were amorphous. In fact, these spheres were subsequently heat treated ( $>1700^{\circ}\text{C}$ ) and gradually crystallized to the hexagonal phase, as determined using SAD. Invariably, crystallization was accompanied with a change of shape from spherical to “platelet” [15].



(a)



(b)

*Figure 6* Sample processed with pure argon plasma at similar operating conditions because typical nitrogen plasma results in no spheroidization. Compare with the image of precursor hBN platelets as in Fig. 1.

The significant differences in outcome between thermal and plasma treatments suggest that the plasma technique is more than simply a superior means to deliver thermal energy. Contrasts in behavior as a function of the identity of the plasma gas support this supposition. In particular, it is notable that spherical particles never formed when precursor BN particles were passed

through pure argon plasmas at exactly the same operating conditions (absorbed power, plasma, and aerosol flow rates) as seen in Fig. 6. The recovered sample maintained the original white coloring while recovered BN processed with a nitrogen plasma was gray to black. In fact, the only modification observed was the formation of agglomerates. The impact of plasma gas

identity on the process provides significant insight into the mechanism for spherodization.

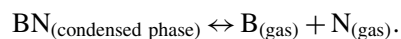
#### 4. Discussion

All of the results obtained in this study can be readily explained by a simple model: platelet and agglomerated BN injected into the plasma melts as it passes through the nitrogen plasma hot zone. Molten BN then forms spheres resulting from surface tension. In the cooler plasma afterglow region, the spherical particles freeze.

The proposition that agglomeration generally takes place before melting is based on the finding that the spheres appear to have a maximum size, a size which is far smaller than that of the largest agglomerates (and 50 times larger than the largest precursor particles). This suggests that agglomerates larger than a certain size simply do not gain enough energy to reach melting temperature. In Fig. 2 (very representative) it is clear that only large agglomerates and spheres smaller than the smallest agglomerate are simultaneously present in the product. If melting of the precursor particles occurred first, particles would grow by the gradual accretion of liquid drops. It is not apparent how this could lead to a maximum sphere size and a minimum agglomerate size. In contrast, the model of agglomeration, followed by the melting of agglomerates below a certain maximum size, is consistent with observation.

This simple model raises several issues. The most obvious is the requirement that BN melt to form a true

liquid. Yet, there is no known atmospheric pressure melting temperature for hexagonal BN because it is one of those materials believed to decompose before melting. A postulate is advanced to explain the character of a nitrogen plasma that allows BN to melt. Specifically, we believe the following equation represents the decomposition-equilibrium:



The temperature of decomposition is thus a strong function of nitrogen-atom pressure [16]. Even in a pure nitrogen ( $\text{N}_2$ ) atmosphere, it is clear that the only source of nitrogen atoms is from the decomposition process. In contrast, there is a high concentration of nitrogen atoms in a nitrogen plasma [17]. Hence, this drives the decomposition-equilibrium reaction back toward the condensed form so that BN is stabilized above the (previously hidden) melting temperature. Further evidence in support of this model is the fact that there is no melting in an argon plasma. This supports the supposition that melting occurs in a nitrogen plasma both because nitrogen atoms are present in excess and a high temperature is reached. Note that neither condition alone is sufficient.

Computations support this model. Assuming the above equilibrium, we computed (Fig. 7) the atomic nitrogen pressure at decomposition temperature [16] from heat of formation and heat capacity data [18–20]. The measured decomposition temperature in the

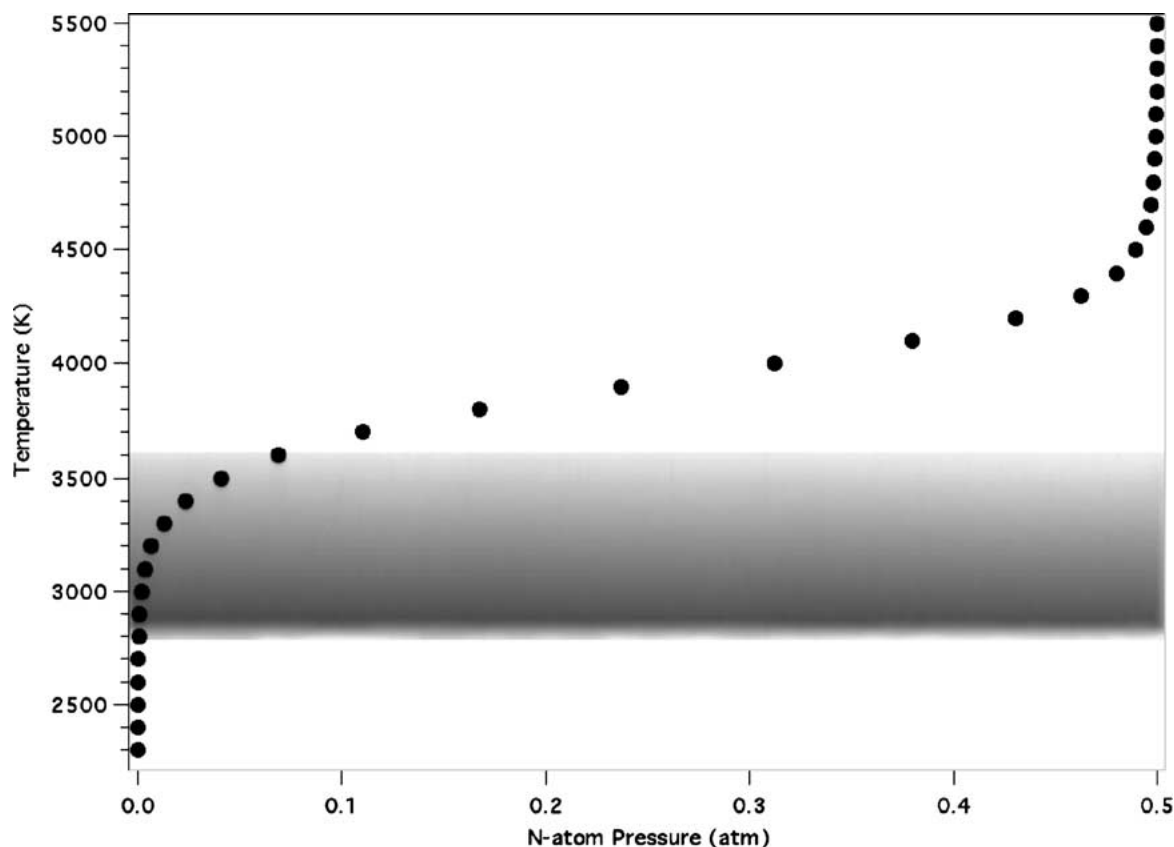


Figure 7 Boron nitride decomposition temperature as a function of N-atom pressure. Because the melting temperature of hBN is not well known, the shaded area from approximately 2800 K is used to denote a possible melting region. Beyond an N-atom pressure of approximately 0.1 atm, the decomposition temperature is elevated significantly beyond the melting temperature. N-atom pressures of 0.25 atm and higher are possible while processing in an atmospheric pressure nitrogen plasma.

absence of any generated N-atoms is reported to be between 2400 to 2600 K [18]. Clearly, in the absence of deliberately generated N-atoms the only source of N-atoms is from the decomposition process, and will be very low. Our computations show the equilibrium decomposition pressure at 2400 K is  $4.7 \times 10^{-6}$  atm., and thus the computation is consistent with the known behavior. The figure shows that generating N-atoms, such as in a nitrogen plasma, will significantly raise the decomposition temperature. For example, the computations indicate that even if less than 10% of the N<sub>2</sub> in an atmospheric pressure plasma is dissociated, the decomposition temperature of BN in the plasma will be raised to about 3600 K. Thus, for example, in an atmospheric N<sub>2</sub> plasma with 10% decomposition, if the melting temperature is higher than 2600 K, likely given the known decomposition behavior, but less than 3500 K, the plasma environment will lead to the melting of BN rather than its decomposition.

Quantification of the fraction of N<sub>2</sub> decomposed is not possible given the available database, although the data do suggest that 10% decomposition is a plausible estimate. Two earlier measures of N-atom concentration in microwave plasma afterglows were made using the NO titration method developed by Campbell and Thrush [21]. In one earlier work [22] with an atmospheric pressure plasma N/N<sub>2</sub> ratios as high as 0.22 were measured 10 cm downstream of the field region. There are several difficulties with using this value in the present work: the position of the spectrometer allowed for significant N-atom recombination prior to measurement, the plasmas studied were mixtures of argon (>95% in all cases) and nitrogen, and the highest power employed was 200 W. In the other earlier study [23] a low pressure pure N<sub>2</sub> plasma (<1 torr) was studied. Although the highest power absorbed was only 250 watts, measurements made 4 cm downstream from the field region indicated that N/N<sub>2</sub> ratios as high as 0.2 were achieved. Both studies clearly showed that the extent of dissociation increased with increases in the absorbed power.

It must be mentioned that the temperature of the plasma is quite high. Completed emission spectroscopy studies (our lab) of the "temperature" of neutrals in the afterglow of an atmospheric pressure argon plasma, generated with the same equipment showed it to be over 3000 K even for only 500 W of applied power and with high flow rates. This value is consistent with that reported by others for low-power, atmospheric pressure systems [24–26]. It should be recognized that the afterglow is not the hottest part of the plasma. The hottest zone encountered by the particles in the aerosol is inside the coupler, and is difficult to probe because of geometric hindrances.

It is seen from the average particle volumes in Table I that certain predictable patterns emerge as a function of operating conditions. For instance, increasing the power causes an increase in particle size, all other factors remaining constant (compare Samples 3 to 2, 2 to 6, and 3 to 6). That is, if the plasma temperature and N-atom concentration were increased, larger agglomerates would melt. If the total gas flow rate is

increased while absorbed power remains constant, the average particle size decreases (compare Samples 4 to 6, 5 to 2, and 5 to 1). This is reasoned as being due to the reduced residence time the particles have in the plasma hot zone. A residence time reduction does not afford agglomerates sufficient time to attain melting temperature regardless of the N atom concentration. If the aerosol gas flow rate is reduced while keeping the two other parameters constant, the particle size is seen to increase. Also, although not reported in Table I, it is seen that an increase in the particle density in the aerosol gas stream causes an increase in the particle size.

## 5. Summary

On the basis of a simple thermodynamic argument we hypothesized and demonstrated a means to melt boron nitride at atmospheric pressure. That is, by dramatically increasing the N atom concentration using an atmospheric pressure plasma the BN decomposition temperature was shifted higher, allowing the previously hidden melting temperature to be reached. This led to the formation of liquid BN particles in the high temperatures found in the plasma (>3000 K) which froze into solid spheres outside the plasma. Spherical BN can be used in place of spherical silica or alumina or even platelet BN as filler for polymers to be used in high heat transfer applications. This may provide the solution to the daunting task of producing high thermal conductivity, low dielectric constant materials, compatible with injection molding techniques. Indeed, spherical BN has long been identified as the filler of choice for "plastic" IC packages. Yet, only platelet shaped BN, which has a dramatically increased mixture viscosity compared to that of spherical BN at the same filler volume fraction in the same polymer at the same temperature, and hence is not compatible with injection molding, is presently available. Finally, it is clear that if this model is correct, it suggests a means to melt a host of materials that at present are only known to decompose. For example, oxides (e.g., AgO<sub>2</sub>) which readily decompose under conventional processing conditions could be stabilized to far higher temperatures in an oxygen plasma, and possibly melted.

## References

1. V. L. VINOGRADOV and A. V. KOSTANOVSKII, *Teplofizika Vysokikh Temperatur* **29** (1991) 1112.
2. P. BUJARD, G. KUHLEIN, S. INO and T. SHIOBARA, *IEEE Trans. Comp., Pack. Manu. Tech. Part A* **17** (1994) 527.
3. V. L. SOLOZHENKO, *Doklady Akademii Nauk SSSR* **301** (1988) 147.
4. *Idem.*, *Thermochimica Acta* **218** (1993) 221.
5. *Idem.*, *Dia. Rel. Mat.* **4** (1994) 1.
6. *Idem.*, *High Press. Res.* **13** (1995) 199.
7. *Idem.*, *J. Hard Mat.* **6** (1995) 51.
8. V. L. SOLOZHENKO, V. Z. TURKEVICH and W. B. HOLZAPFEL, *J. Phys. Chem.* **B 103** (1999) 2903.
9. R. H. WENTORF JR., *J. Phys. Chem.* **38** (1959) 1934.
10. H. SHIM, J. PHILLIPS and I. SILVA, *J. Mat. Res.* **14** (1999) 849.
11. J. PHILLIPS, US Patent no 5989648.
12. J. PHILLIPS, S. GLEIMAN and C-K. CHEN, US Patent no. 6261484.

13. C-K. CHEN, S. S. GLEIMAN and J. PHILLIPS, *J. Mater. Res.* **16** (2001) 1256.
14. Advanced Ceramics Corporation, Cosmetic Ceramic Boron Nitride Powder, Grade CC6004.
15. Private communication.
16. S. I. SANDLER, in "Chemical and Engineering Thermodynamic," 2nd edn. (Wiley, New York, 1989) p. 494.
17. A. M. DIAMN, J. C. LEGRAND, A. MORITTS and A. RICARD, *Surf. Coat. Tech.* **112** (1999) 38.
18. I. BARIN, in "Thermochemical Data of Pure Substances," 3rd edn. (VCH, New York, 1996) p. 104 and 121.
19. J. D. COX, D. D. WAGMAN and V. A. MEDVEDEV (eds.), in "CODATA Key Values for Thermodynamics" (Hemisphere Publishing Corporations, New York, 1989) p. 187 and 212.
20. M. W. CHASE JR. *et al.*, in "JANAF Thermochemical Tables," 3rd edn. (ACS Publishing, New York, 1989) p. 175 and 246.
21. G. MANNELLA, *Chem. Rev.* **63** (1963) 1.
22. A. RICARD, A. BESNER, J. HUBERT and M. MOISON, *J. Phys. B* **21** (1988) L579.
23. T. C. WEI, L. R. COLLINS and J. PHILLIPS, *AIChE J* **42** (1996) 1361.
24. C. O. LAUX *et al.*, *J. Quant. Spectro. Rad. Trans.* **68** (2001) 473.
25. J. M. BADIE, P. BERTRAND and G. FLAMANT, *Plasma Chem. Plasma Proc.* **21** (2001) 279.
26. J. HUGILL and T. SAKTIOTO, *Plasma Sources Sci. Tech.* **10** (2001) 38.

*Received 23 August 2001  
and accepted 29 March 2002*